WEISKOPF & PICKWORTH
CONSULTING ENGINEERS
45 WEST 45th STREET, N. Y. C.

Job No.
Designed by
Sheet No. of
Date 9-1-49

FLEXURE OF I SECTIONS ABOVE THE ELASTIC RANGE

by

Walter H. Weiskopf

INTRODUCTION

For I sections in flexure in the elastic range the familiar expression $\frac{d^2y}{dx^2} = \frac{M}{EI}$ applies, and its integrations provide the slope, the deflection curve, and the solutions of innumerable bending problems. It is the purpose of this paper to develop corresponding equations for I sections in the plastic and strain-hardening ranges. The results are then compared with measurements of beams in flexure as given in the paper "Plastic Behavior of Continuous Beams, Progress Report B", Fritz Engineering Laboratory, Lehigh University, dated May 26, 1949.

The Plastic and Strain-Hardening Ranges

Fig. 1, which is a reproduction of Fig. 50 of Progress Report B, clearly shows the elastic, plastic, and strain-hardening ranges of a specimen in tension. In flexure, however, the situation is not so simple. As the load increases some of the fibres distant from the neutral axis, and where the bending moment is great, enter the plastic range. There is then a portion of the beam in the elastic range and a portion, usually smaller, in the plastic range.

As the load is further increased some of the fibres enter the strain-hardening range, and there are then three portions of beam, one still elastic, a second in the plastic and a third in the strain-hardening range. Progress Report B shows that for I sections some of the fibres enter the strain-hardening range before failure. If the beam is statically indeterminate another portion may enter the plastic range and thus relieve the portions near the maximum bending moment. Theory, as well as Progress Report B, indicate that the fibres near the maximum bending moment often enter the strain-hardening range and may fail before other portions become plastic and cause a redistribution of bending moments. In this respect the so-called "Theory of Limit Design" appears to be in error.

The Plastic Range

The stress-strain diagram is idealized as shown in Fig. 2. Applied to an I section in flexure the strain and stress diagrams are shown in Figs. 3a and 3b. From Fig. 3a it is seen that the rotation per unit length of beam is

$$\phi = \frac{\sigma_y}{E y_0} \qquad (1)$$

Taking moments about the neutral axis in Fig. 3b there is obtained

$$M = \sigma_y \left(\frac{I_E}{y_0} + Z - Z_E \right) \qquad (2)$$

In this expression I_E is the moment of inertia and Z_E is the statical moment of the elastic portion of the cross section and Z is the statical moment of the entire cross section.

When the value of y_0 is such that the elastic portion of the cross section is entirely in the web equation (2) becomes

$$M = \sigma_y \left(Z - \frac{y_0^2 t}{3} \right) \qquad (3)$$

In equation (3) t is the web thickness.

Eliminating y_0 from equations (1) and (3)

$$\phi = \frac{\sigma_y}{E} \sqrt{\frac{\sigma_y t}{3(\sigma_y Z - M)}} \qquad (4)$$

In equation (4) the expression $\sigma_y Z$ is the limiting value of the bending moment in which all of the fibres are stressed to the yield point as shown in Fig. 3c. Let $M_z = \sigma_y Z$

Then equation (4) becomes

$$\phi = \frac{\sigma_y}{E}\sqrt{\frac{\sigma_y t}{3(M_z - M)}} \qquad (5)$$

This is the fundamental relation of M to ϕ for the plastic range. In Fig. (4) this relation is plotted for an 8 WF 40. From the origin to point 1 the beam is elastic. From point 1 to point 2, y_o is in the flange or fillet. To the right of point 2, y_o is in the web and equation (5) applies. The portion 1 to 2 is a small portion of the useful range. To simplify the mathematics equation (5) will be extended to the left until it meets an extension of the elastic range at point 4. The value of the resisting moment at point 4, M_o, can be found by treating equation (5) simultaneously with the elastic expression $\phi = M/EI$

$$3M_o^3 - 3M_z M_o^2 + I^2\sigma_y^3 t = 0 \qquad (6)$$

M_o can be found by solving equation (6). It is a function of the cross section and σ_y only and can be tabulated for all beam sizes.

For the remainder of this paper the elastic range will be taken from zero moment to M_o and the plastic range from M_o to M_z.

<u>Integrating the M-ϕ Curve. (Plastic Range)</u>

As is usually assumed in the theory of flexure, $\frac{d^2y}{dx^2}$ is taken equal to ϕ and equation (5) becomes

$$\frac{d^2y}{dx^2} = \frac{\sigma_y}{E}\sqrt{\frac{\sigma_y t}{3(M_z - M)}} \qquad (6a)$$

This expression must be integrated along the length of the beam in the plastic range. For this integration M is a function of x and the remainder of the right hand side of equation (6a) is constant. The integrations have been performed for three cases: Fig. (5), the bending moment, M , is constant; Fig. (6) M follows a straight line variation (as between concentrated loads); Fig. (7) M follows a parabolic diagram (as for a uniform load). In these expressions, ℓ is the length of the plastic portion which is generally only a small part of the total length of the beam.

The expressions first give the slope, $\frac{dy}{dx}$, and the deflection, y , at any point in the length. The constants of integration have been determined so as to give values in terms of the bending moments at the ends and the slope, α_L , and deflection , y_L , at the left end. Next (making $x = \ell$) the slope, α_R , and deflection , y_R , at the right end are obtained. Finally expressions for α_R and y_R are given for the special case, $M_L = M_I$, that is the full plastic range.

The Strain-hardening Range

Above the plastic range the stress-strain curve again rises as shown in Fig. 1. It is assumed that the diagram follows a straight line in the strain-hardening range given by the equation

$$\sigma = B\epsilon + A \qquad (26)$$

B and A are constants of the material, B being analagous to E in the elastic range. For the steel shown in Fig. 1, B equals 667 and A equals 28 kips per square inch. Fig. 8 represents the strain and stress diagrams for an I beam. From the figure

$$f = \frac{\sigma_y - A}{\sigma - A} c \qquad (27)$$

When the distance, f , is entirely in the web, the resisting moment of the cross section is

$$M = AZ + (\sigma - A)\frac{I}{c} + \frac{1}{3}(\sigma_y - A) t f^2 \qquad (28)$$

In the right hand member of equation (28) the first term covers the rectangle 0, 1, 4, 3; the second term the triangle 1, 5, 4 and the third term the triangle 1, 2, 6. Computations have shown this last term to be very small. If it is neglected equation (28) becomes

$$M = AZ + (\sigma - A)\frac{I}{c} \qquad (29)$$

From Fig. 8

$$\phi = \frac{\epsilon}{c} = \frac{\sigma - A}{Bc} \qquad (30)$$

Substituting $\sigma - A$ from equation (29) into (30)

$$\phi = \frac{d^2y}{dx^2} = \frac{M - AZ}{BI} \qquad (31)$$

In Fig. 9 the relation of M to ϕ for an 8 WF 40 is again shown. This is similar to Fig. 4, but extended into the strain-hardening range. The solid line is the theoretical curve and the dotted line is equation (31).

It has been found that failure takes place before the stress gets very far into the strain-hardening range. Using the approximation of equation (31) therefore appears well justified.

In integrating equation (31) M is a function of x and the remaining symbols are constants. The integrations are so simple that they can be performed for each case without difficulty and will not be given here.

Numerical Example

To illustrate the method it will be applied to a beam with fixed ends and loads at the third points. This is Test No. B2 of Progress Report B, and is shown in Fig. 10. The following values are used:

8 WF 40

$I = 146.3$ $\quad A = 28$

$S = 35.5$ $\quad B = 667$

$Z = 39.8$ $\quad l = 168$

$t = .365$

σ_y is taken as 37.6 which is an average value of the test Coupon Results, Table I of Progress Report B.

$M_y = 35.5 \times 37.6 = 1335''^k$

$M_z = 39.8 \times 37.6 = 1500''^k$

From equation (6)

$$3 M_0^3 - 3 \times 1500 M_0^2 + 146.3^2 \times 37.6^3 \times .365 = 0$$

Solving this $M_0 = 1433''^k$

In the elastic range the fixed end moment is $\frac{2Pl}{9}$ and the center moment $\frac{Pl}{9}$.

Then $\frac{2Pl}{9} = M_0$

$$P = \frac{9 M_0}{2 l} = \frac{9 \times 1433}{2 \times 168} = 38.4^k$$

This is the limiting load for the elastic range. For greater loads the ends of the beam enter the plastic range. The bending moment diagram for this condition is shown in Fig. 10b. The plastic section extends from the left and to the point where the bending moment equals M_0. The coordinate of this point is x_0. Treating the center section of the beam and the elastic portion of the left section (where x is greater than x_0) an expression for the slope can be found by the usual elastic theory. This is

$$\frac{dy}{dx} = \frac{1}{EI}\left[M_F\left(x - \frac{l}{2}\right) + P\left(\frac{l^2}{9} - \frac{x^2}{2}\right)\right] \qquad (32)$$

The fixed end moment M_F is of course not the same as when the beam is entirely in the elastic range. In equation (32) it is unknown.

The slope where the elastic portion meets the plastic portion is found by putting x_0, for x in equation (32).

$$\frac{dy}{dx}_0 = \frac{1}{EI}\left[M_F\left(x_0 - \frac{l}{2}\right) + P\left(\frac{l^2}{9} - \frac{x_0^2}{2}\right)\right] \qquad (33)$$

The slope at this point working from the left end of the beam through the plastic portion can be found by putting the proper values in equation (15). α_L equals zero since the beam is fixed at the end. For M_R put M_0 and for M_L put M_F. For l put x_0

Then

$$\alpha_R = \frac{2\sigma_y}{E}\sqrt{\frac{\sigma_y t}{3}} \times \frac{x_0}{M_F - M_0}\left[\sqrt{M_z - M_0} - \sqrt{M_z - M_F}\right] \qquad (34)$$

Obviously $\frac{dy}{dx}_0$ of equation (33) must equal α_R of equation (34). Equating gives an expression in which x_0 and M_F are unknown. From Fig. 10

$$x_0 = \frac{M_F - M_0}{P} \qquad (35)$$

Substituting this in equations (33) and (34) equating the values, and simplifying there is obtained

$$\frac{2I\sigma_y}{P}\sqrt{\frac{\sigma_y t}{3}}\left[\sqrt{M_z - M_0} - \sqrt{M_z - M_F}\right] = \frac{M_F^2 - M_0^2}{2P} - \frac{M_F l}{2} + \frac{Pl^2}{9} \qquad (36)$$

For any load, P, equation (36) can be solved for the fixed and moment, M_F, by trial.

The largest value that P can have within the plastic range is that which makes the fixed end moment, M_F, equal to M_z. This can be obtained by making M_F equal to M_z in equation (36) and solving for P. The resulting equation is a quadratic and its solution is

$$P = \frac{9M_z}{4\ell} \pm \frac{3}{\ell}\sqrt{\frac{M_z^2}{16} + \frac{M_0^2}{2} + 2I\sigma_y\sqrt{\frac{\sigma_y t}{3}}(M_z - M_0)} \qquad (37)$$

For the numerical example in Fig. 10 equation (37) gives $P = 41.0^k$ and $x_0 = 1.63''$. This is the greatest value P can have before the fibres near the end of the beam enter the strain-hardening range. For this value of P the moment at the center of the beam is $800''^k$, well within the elastic range.

For values of P greater than 41.0^k the strain-hardening range is entered and the condition is that shown in Fig. 10c. The bending moment at any point in the end third is of course

$$M = M_F - Px \qquad (38)$$

From the figure the following relations can be obtained:

$$x_0 = \frac{M_F - M_0}{P} \qquad (39)$$

$$x_z = \frac{M_F - M_z}{P} \qquad (40)$$

$$x_0 - x_z = \frac{M_z - M_0}{P} \qquad (41)$$

The slope at any point on the elastic portion of the end third of the beam is again given by equation (32). The slope when x equals x_0 can be found by putting x_0 for x in this equation. Then using the value of x_0 as given in equation (39)

$$\frac{dy}{dx}_0 = \frac{1}{EI}\left[\frac{M_F^2 - M_0^2}{2P} - \frac{M_F\ell}{2} + \frac{P\ell^2}{9}\right] \qquad (42)$$

For the plastic section equation (17) applies. α_R is given by equation (42) and M_R is M_o. ℓ is $\frac{M_z \cdot M_o}{P}$ as given by equation (41).

$$\alpha_L = -\frac{2\sigma_y}{E}\sqrt{\frac{\sigma_y t}{3}} \times \sqrt{\frac{M_z - M_o}{P}} + \frac{1}{EI}\left[\frac{M_F^2 - M_o^2}{2P} - \frac{M_F \ell}{2} + \frac{P\ell^2}{9}\right] \quad (43)$$

In the strain-hardening section, from equation (38)

$$\frac{d^2y}{dx^2} = \frac{M - AZ}{BI} = \frac{1}{BI}\left[M_F - Px - AZ\right] \quad (44)$$

Integrating

$$\frac{dy}{dx} = \frac{1}{BI}\left[M_F x - \frac{Px^2}{2} - AZx + C\right] \quad (45)$$

From the condition that $\frac{dy}{dx} = 0$ when $x = 0$ it is seen that the constant of integration, C, equals zero.

Putting x_z for x in equation (45) gives the slope where the plastic and strain-hardening sections meet. At this point, from (45) and (40)

$$\frac{dy}{dx} = \frac{1}{2BIP}\left[M_F^2 - M_z^2 - 2AZ(M_F - M_z)\right] \quad (46)$$

The slopes as given by equations (46) and (43) must be the same. Equating them gives an expression that can be solved for M_F. It is

$$\left(-\frac{1}{B} + \frac{1}{E}\right)\frac{M_F^2}{2I} + \left(\frac{AZ}{BI} - \frac{P\ell}{2EI}\right)M_F - \frac{M_o^2}{2EI} + \frac{M_z^2}{2BI} + \frac{P^2\ell^2}{9EI} - \frac{AZM_z}{BI} - \frac{2\sigma_y}{E}\sqrt{\frac{\sigma_y t}{3}}\sqrt{M_z - M_o} = 0 \quad (47)$$

This is a quadratic and values of M_F can be computed without difficulty.

P	M_F
45^k	$1525^{''k}$
50	1565
55	1606

Once M_F is known the deflections can be easily found by integrating equations (32) for the elastic portion, (45) for the strain-hardening portion and using equation (18) for the plastic portion.

Comparison of Numerical Results with Progress Report B

Figs. 11 and 12 are reproductions of Figs. 10 and 11 of Progress Report B. These show M-ϕ curves for an 8 WF 40 beam. Values based on equation (5) of this paper (marked WHW values) are also shown. They come between the theoretical curve calculated in Progress Report B and the experimental curve.

Fig. 13 (a reproduction of Fig. 12 of Progress Report B) shows the deflection at the center of a simply supported 8 WF 40 loaded at the third points. Values obtained by applying the analysis here presented again are shown.

Fig. 14, which is a reproduction of Fig. 19 of Progress Report B, shows the measured moments at the ends and at the center of a beam fixed at the ends and loaded at the third points. This is the numerical example previously given. Measurements extended through the elastic, plastic and strain-hardening ranges. The WHW values again are plotted. These values were taken up to the point where the center moment enters the plastic range.

Beyond this point the end moments would turn upward and the center moment would flatten again agreeing with the measurements.

Fig. 15, a reproduction of Fig. 15 of Progress Report B, shows center deflections for the same beam. Again the WHW values have been computed up to the point where the center moment enters the plastic range. Beyond this point the curves would become almost horizontal. The agreement between measured and WHW values here is not as good as in previous cases, the WHW deflections being too small. It is believed that the reason for this is that the theory here presented takes into account flexural deflections only and disregards shearing deflections. For a beam with loads at the third points and such great loads, the shearing deflections are probably material and when added to the WHW values would give a much closer check.

Bending about the Weak Axis

For I sections subject to flexure about the weak axis all of the equations for the plastic range (Figs. 5, 6 and 7) can be used, if for the web thickness, t, twice the flange thickness is used. As a matter of fact, these equations can also be used for rectangular sections if the width of the beam is used instead of the web thickness, t. The strain-hardening equations do not apply as accurately to the weak axis or to rectangular shapes. As a matter of fact, however, failure about the weak axis or in rectangular shapes is apt to take place before going far into the strain-hardening range if at all, so that for these cases M_z could be considered the ultimate bending moment.

CONCLUSION

The expressions derived in this paper appear to check satisfactorily with the measurements of Progress Report B for the few cases tried. If further comparisons also show a good agreement, this method could be used for the plastic and strain-hardening ranges, as the usual theory of flexure is used for the elastic range. While too complicated for ordinary design purposes the method is suggested as a new tool for the research program.

NOTATION

A, B	Constants of the material in the strain-hardening range.
c	One half the depth of the beam.
E	Modulus of elasticity.
f	Portion of beam depth (See Fig. 8).
I	Moment of inertia of entire cross section.
I_E	Moment of inertia of elastic portion of cross section.
l	Length of beam or portion of beam.
M	Bending moment.
M_F	Fixed end moment.
M_y	Bending moment at yield point.
M_o	Bending moment at limit of elastic range as assumed in this paper.
M_z	Bending moment at limit of plastic range.
M_L	Bending moment at left end of portion of beam.
M_R	Bending moment at right end of portion of beam.
P	Load on beam.
S	Section modulus.
t	Thickness of web.
x, y	Coordinates
x_o, x_z	Portions of beam length (See Fig. 10).
y_o	Portion of beam depth (See Fig. 3).
Z	Statical moment of entire cross section.
Z_E	Statical moment of elastic portion of cross section.

NOTATION (continued)

α Slope of neutral surface of beam at any point.

α_R Slope of neutral surface at right of section considered.

α_L Slope of neutral surface at left of section considered.

ϵ Strain

ϕ Angular rotation in beam per unit length.

σ Stress

σ_y Yield point stress.

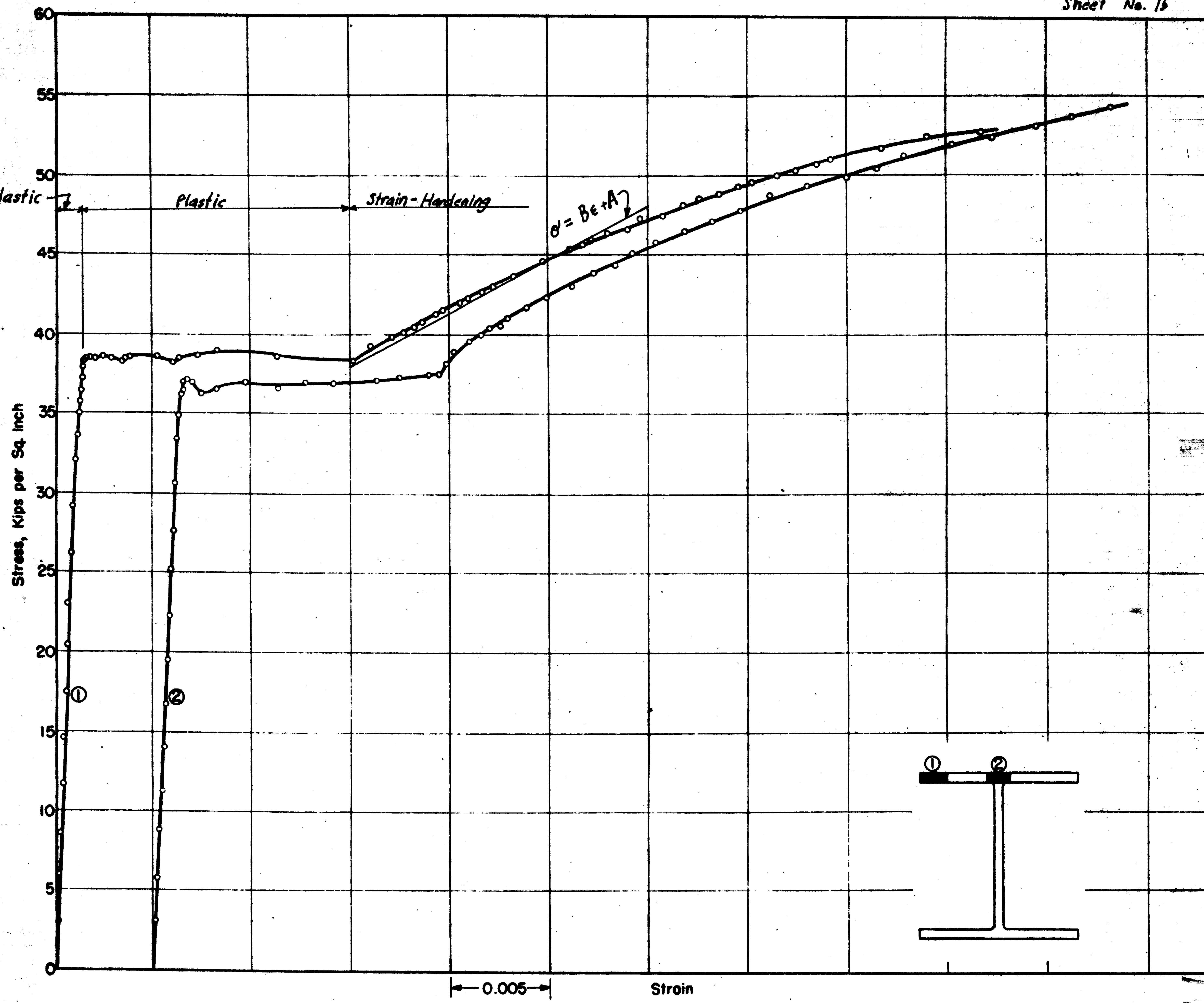

FIG. 1. TENSION STRESS-STRAIN CURVES FOR AN 8WF40 BEAM
(Including strain-hardening range)

WEISKOPF & PICKWORTH
CONSULTING ENGINEERS
45 WEST 45th STREET, N. Y. C.

Job No.
Designed by
Sheet No. 16 of
Date

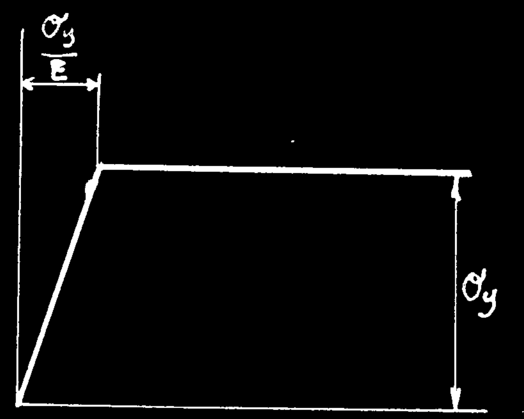

Fig. 2.

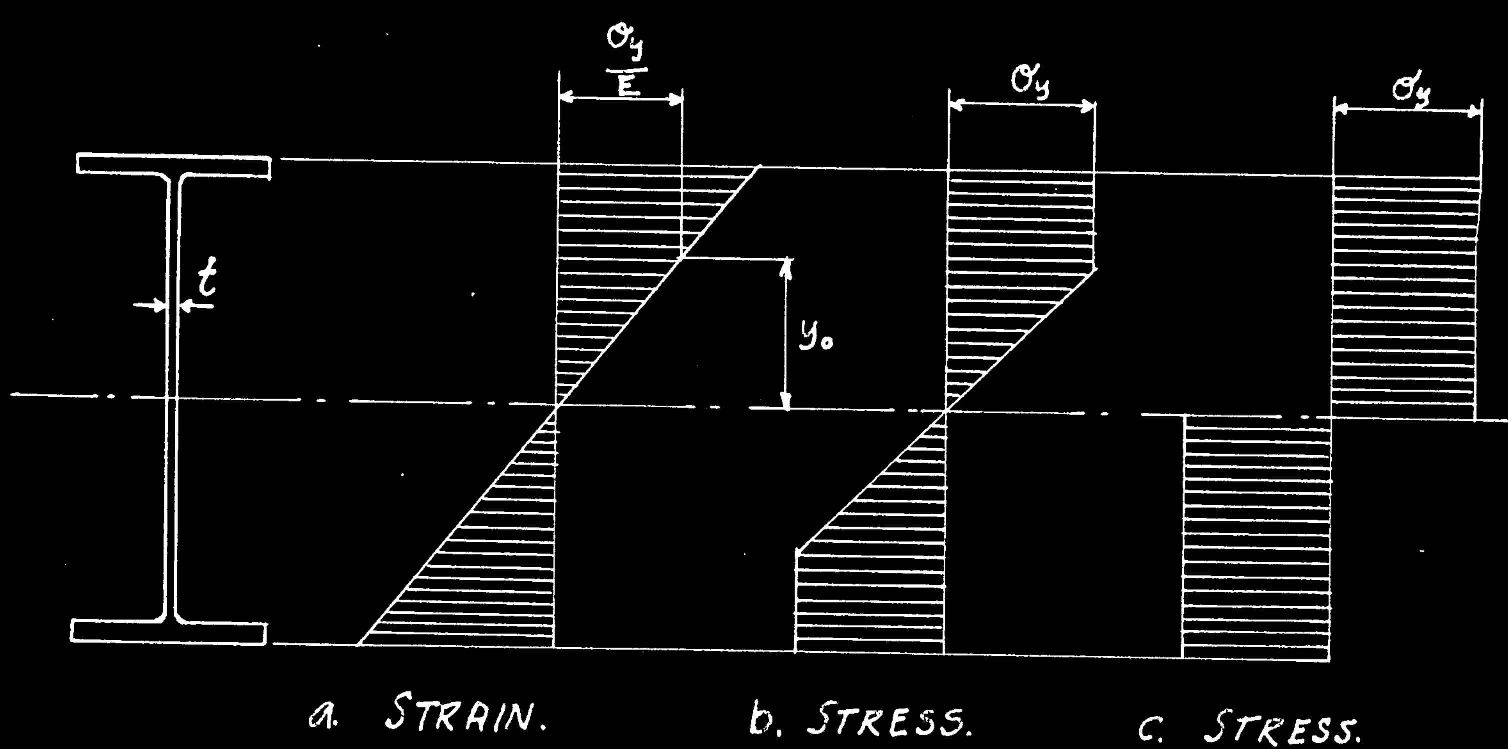

Fig. 3

WEISKOPF & PICKWORTH
CONSULTING ENGINEERS
45 WEST 45th STREET, N. Y. C.

Job No.
Designed by
Sheet No. 17 of
Date

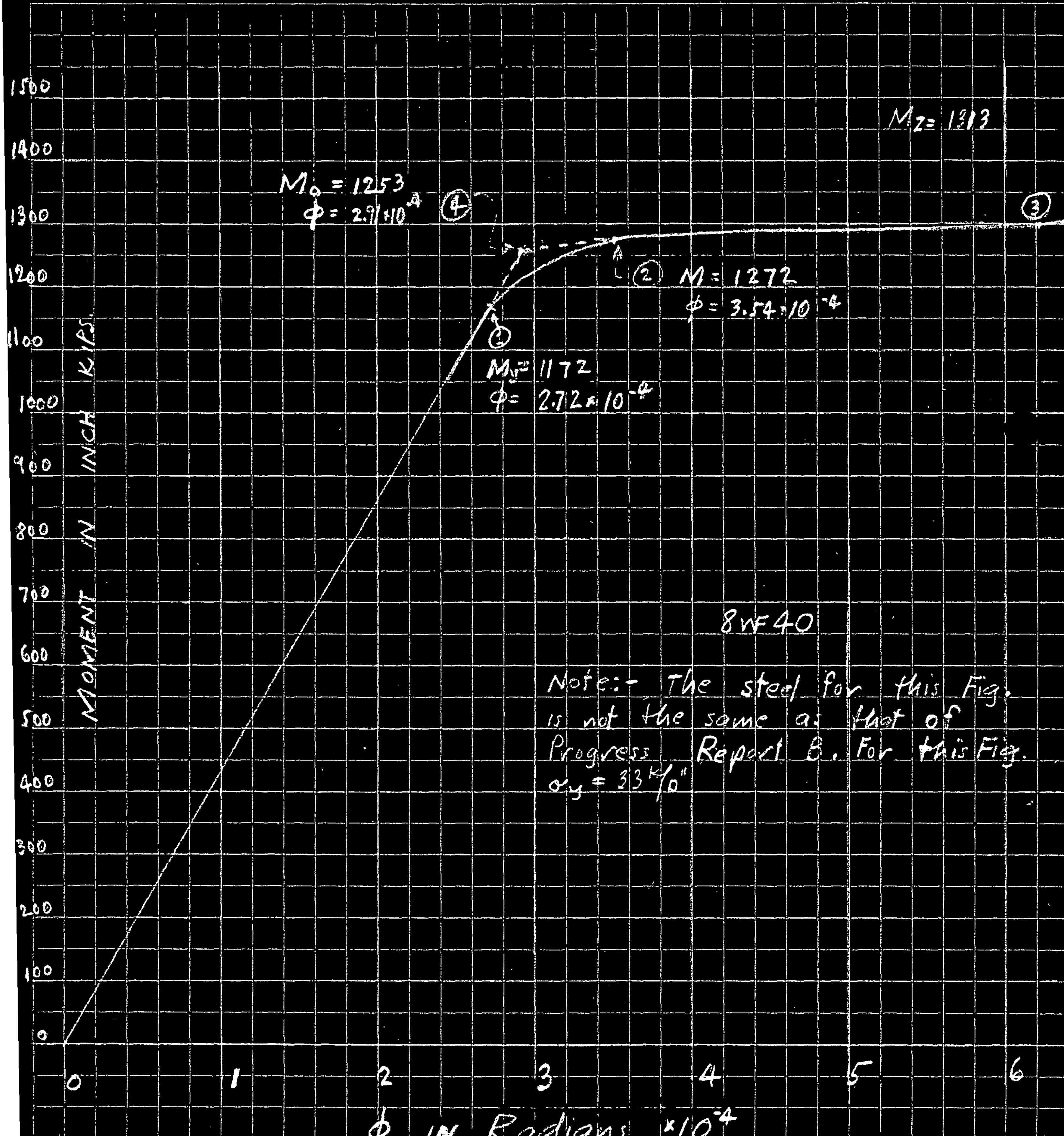

Fig. 4

CONSTANT MOMENT

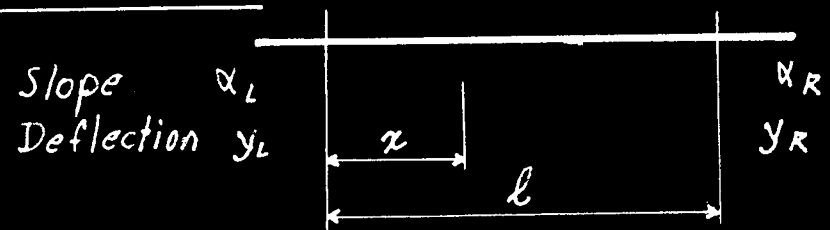

$$\frac{d^2y}{dx^2} = \frac{\sigma_y}{E}\sqrt{\frac{\sigma_y t}{3(M_z - M)}} \qquad (7)$$

$$\frac{dy}{dx} = \frac{\sigma_y}{E}\sqrt{\frac{\sigma_y t}{3(M_z - M)}} \times x + \alpha_L \qquad (8)$$

$$y = \frac{\sigma_y}{E}\sqrt{\frac{\sigma_y t}{3(M_z - M)}} \times \frac{x^2}{2} + \alpha_L x + y_L \qquad (9)$$

For full length $(x = \ell)$

$$\alpha_R = \frac{\sigma_y}{E}\sqrt{\frac{\sigma_y t}{3(M_z - M)}} \times \ell + \alpha_L \qquad (10)$$

$$y_R = \frac{\sigma_y}{E}\sqrt{\frac{\sigma_y t}{3(M_z - M)}} \times \frac{\ell^2}{2} + \alpha_L \ell + y_L \qquad (11)$$

Fig. 5.

WEISKOPF & PICKWORTH
CONSULTING ENGINEERS
45 WEST 45th STREET, N. Y. C

Job No.
Designed by
Sheet No. 19 of
Date

STRAIGHT LINE MOMENT DIAGRAM

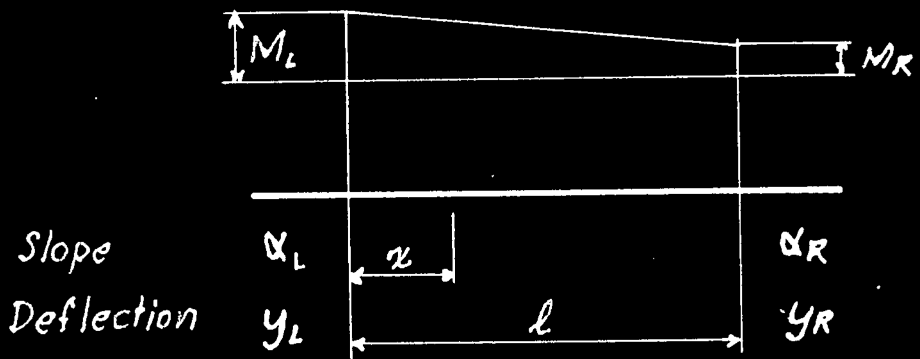

$$\frac{d^2y}{dx^2} = \frac{\sigma_y}{E}\sqrt{\frac{\sigma_y t}{3}} \times \frac{1}{\sqrt{M_z - M_L + (M_L - M_R)x/\ell}} \qquad (12)$$

$$\frac{dy}{dx} = \frac{2\sigma_y}{E}\sqrt{\frac{\sigma_y t}{3}} \times \frac{\ell}{M_L - M_R}\left[\sqrt{M_z - M_L + (M_L - M_R)\frac{x}{\ell}} - \sqrt{M_z - M_L}\right] + \alpha_L \qquad (13)$$

$$y = \frac{4\sigma_y}{3E}\sqrt{\frac{\sigma_y t}{3}} \times \frac{\ell^2}{(M_L - M_R)^2}\left\{\left[M_z - M_L + (M_L - M_R)\frac{x}{\ell}\right]^{\frac{3}{2}} - \left[M_z - M_L\right]^{\frac{3}{2}}\right\}$$

$$- \frac{2\sigma_y}{E}\sqrt{\frac{\sigma_y t}{3}} \times \frac{\ell x}{M_L - M_R}\sqrt{M_z - M_L} + \alpha_L x + y_L \qquad (14)$$

For full length ($x = \ell$)

$$\alpha_R = \frac{2\sigma_y}{E}\sqrt{\frac{\sigma_y t}{3}} \times \frac{\ell}{M_L - M_R}\left[\sqrt{M_z - M_R} - \sqrt{M_z - M_L}\right] + \alpha_L \qquad (15)$$

$$y_R = \frac{4\sigma_y}{3E}\sqrt{\frac{\sigma_y t}{3}} \times \frac{\ell^2}{(M_L - M_R)^2}\left[(M_z - M_R)^{\frac{3}{2}} - (M_z - M_L)^{\frac{3}{2}}\right] - \frac{2\sigma_y}{E}\sqrt{\frac{\sigma_y t}{3}} \times \frac{\ell^2}{M_L - M_R}\sqrt{M_z - M_L}$$

$$+ \alpha_L \ell + y_L \qquad (16)$$

When $M_L = M_z$

$$\alpha_R = \frac{2\sigma_y}{E}\sqrt{\frac{\sigma_y t}{3}} \times \frac{\ell}{\sqrt{M_z - M_R}} + \alpha_L \qquad (17)$$

$$y_R = \frac{4\sigma_y}{3E}\sqrt{\frac{\sigma_y t}{3}} \times \frac{\ell^2}{\sqrt{M_z - M_R}} + \alpha_L \ell + y_L \qquad (18)$$

Fig 6.

PARABOLIC MOMENT DIAGRAM

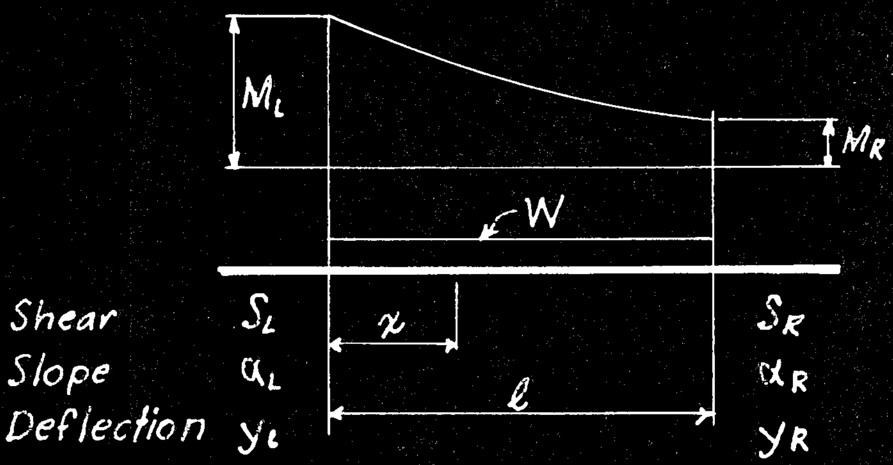

$$S_L = \frac{M_R - M_L}{\ell} - \frac{W\ell}{2}$$

$$S_R = \frac{M_R - M_L}{\ell} + \frac{W\ell}{2}$$

$$\frac{d^2y}{dx^2} = \frac{\sigma_y}{E}\sqrt{\frac{\sigma_y t}{3}}\;\frac{1}{\sqrt{M_z - M_L - S_L x - \frac{Wx^2}{2}}} \qquad (19)$$

$$\frac{dy}{dx} = \frac{\sigma_y}{E}\sqrt{\frac{2\sigma_y t}{3W}}\left[\sin^{-1}\frac{Wx + S_L}{\sqrt{2W(M_z - M_L) + S_L^2}} - \sin^{-1}\frac{S_L}{\sqrt{2W(M_z - M_L) + S_L^2}}\right] + \alpha_L \qquad (20)$$

$$y = \frac{\sigma_y}{E}\sqrt{\frac{2\sigma_y t}{3W}}\left[\frac{Wx + S_L}{W}\sin^{-1}\frac{Wx + S_L}{\sqrt{2W(M_z - M_L) + S_L^2}} - \frac{Wx + S_L}{W}\sin^{-1}\frac{S_L}{\sqrt{2W(M_z - M_L) + S_L^2}}\right.$$
$$\left. + \sqrt{\frac{2(M_z - M_L)}{W} - x^2 - \frac{2S_L x}{W}} - \sqrt{\frac{2(M_z - M_L)}{W}}\right] + \alpha_L x + y_L \qquad (21)$$

For full length $(x = \ell)$

$$\alpha_R = \frac{\sigma_y}{E}\sqrt{\frac{2\sigma_y t}{3W}}\left[\sin^{-1}\frac{S_R}{\sqrt{2W(M_z - M_L) + S_L^2}} - \sin^{-1}\frac{S_L}{\sqrt{2W(M_z - M_L) + S_L^2}}\right] + \alpha_L \qquad (22)$$

$$y_R = \frac{\sigma_y}{E}\sqrt{\frac{2\sigma_y t}{3W}}\left[\frac{S_R}{W}\sin^{-1}\frac{S_R}{\sqrt{2W(M_z - M_L) + S_L^2}} - \frac{S_R}{W}\sin^{-1}\frac{S_L}{\sqrt{2W(M_z - M_L) + S_L^2}}\right.$$
$$\left. + \sqrt{\frac{2(M_z - M_R)}{W}} - \sqrt{\frac{2(M_z - M_L)}{W}}\right] + \alpha_L \ell + y_L \qquad (23)$$

Fig. 7

When $M_L = M_I$

$$\alpha_R = \frac{\sigma_y}{E}\sqrt{\frac{2\sigma_y t}{3W}}\left[\sin^{-1}\frac{S_R}{S_L} - \frac{\pi}{2}\right] + \alpha_L \quad (24)$$

$$y_R = \frac{\sigma_y}{E}\sqrt{\frac{2\sigma_y t}{3W}}\left[\frac{S_R}{W}\sin^{-1}\frac{S_R}{S_L} - \frac{\pi S_R}{2W} + \sqrt{\frac{2(M_I - M_R)}{W}}\right] + \alpha_L l + y_L \quad (25)$$

Fig. 7
(CONTINUED)

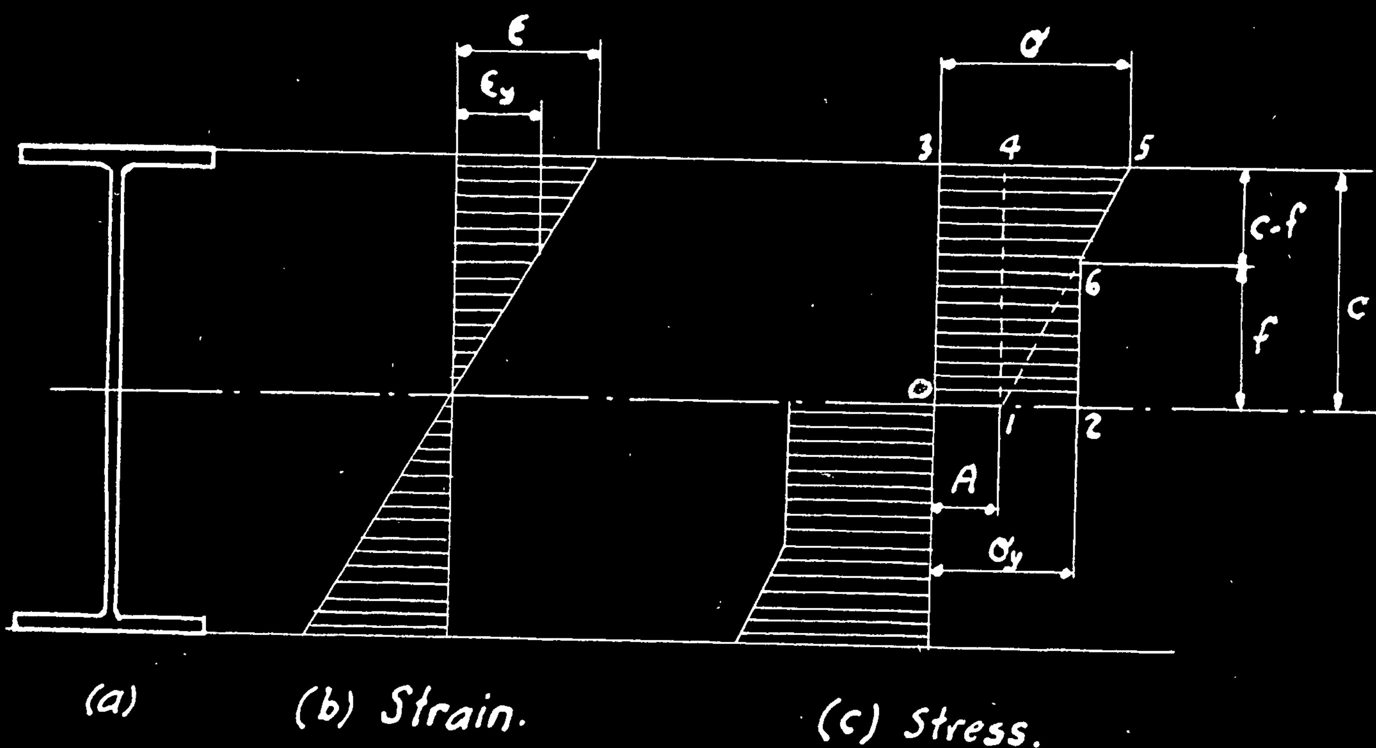

Fig. 8

WEISKOPF & PICKWORTH
CONSULTING ENGINEERS
45 WEST 45th STREET, N. Y. C.

Job No. ....
Designed by ....
Sheet No. 23 of ....
Date ....

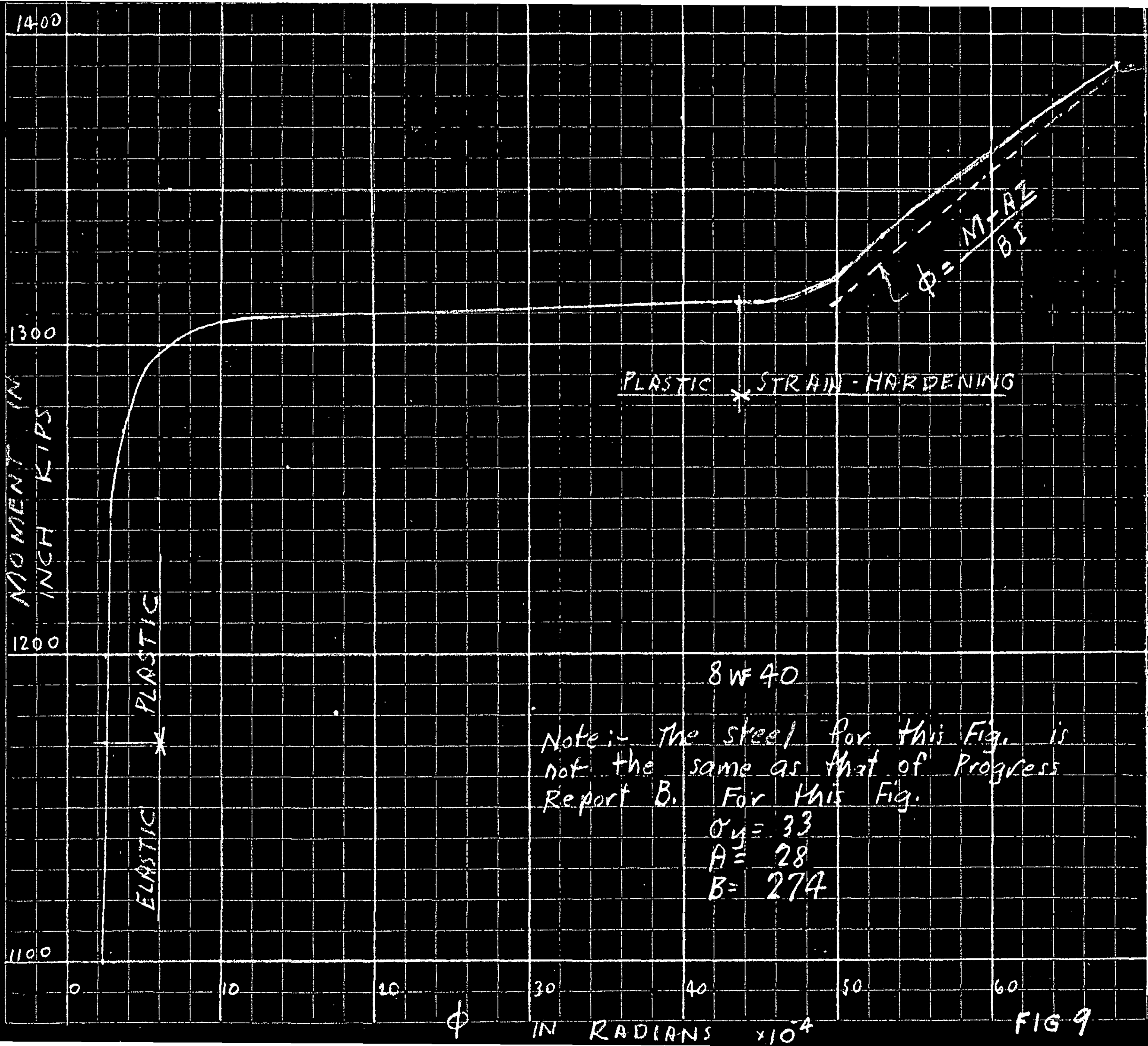

FIG 9

WEISKOPF & PICKWORTH
CONSULTING ENGINEERS
45 WEST 45th STREET, N. Y. C.

Job No. ______
Designed by ______
Sheet No. 24 of ______
Date ______

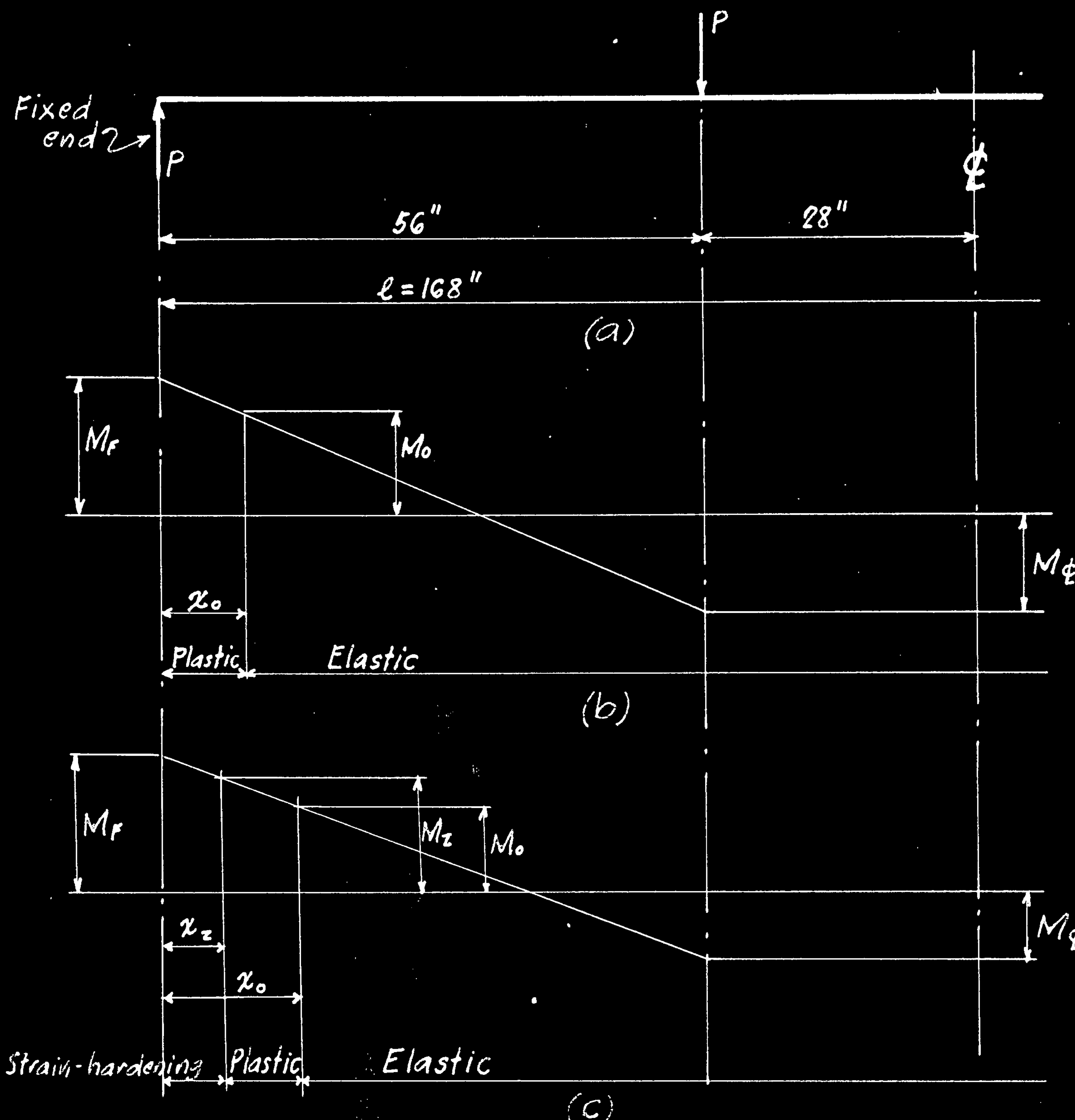

Fig. 10

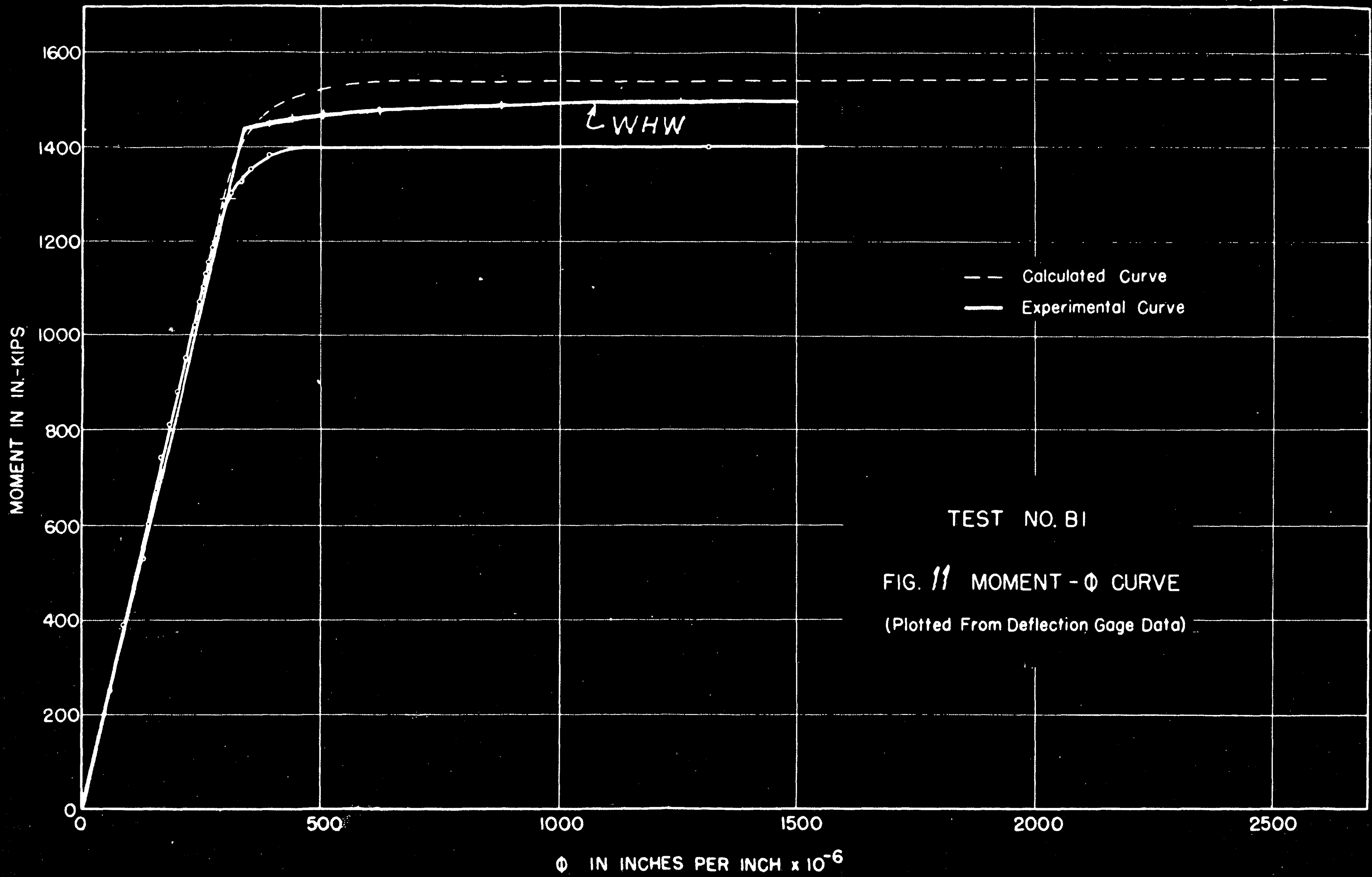

TEST NO. B1

FIG. 11 MOMENT - Φ CURVE

(Plotted From Deflection Gage Data)

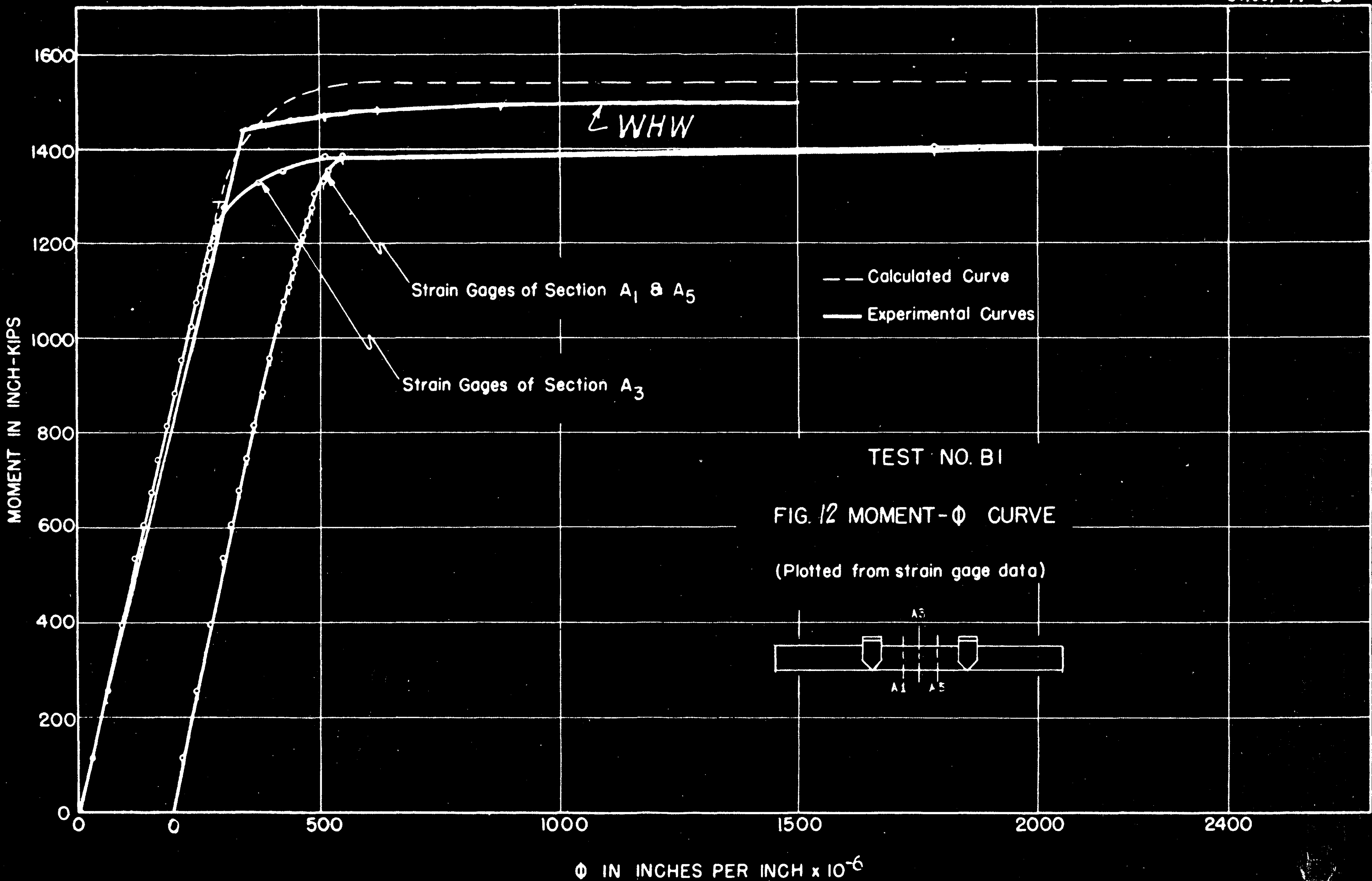

TEST NO. B1

FIG. 12 MOMENT-Φ CURVE

(Plotted from strain gage data)

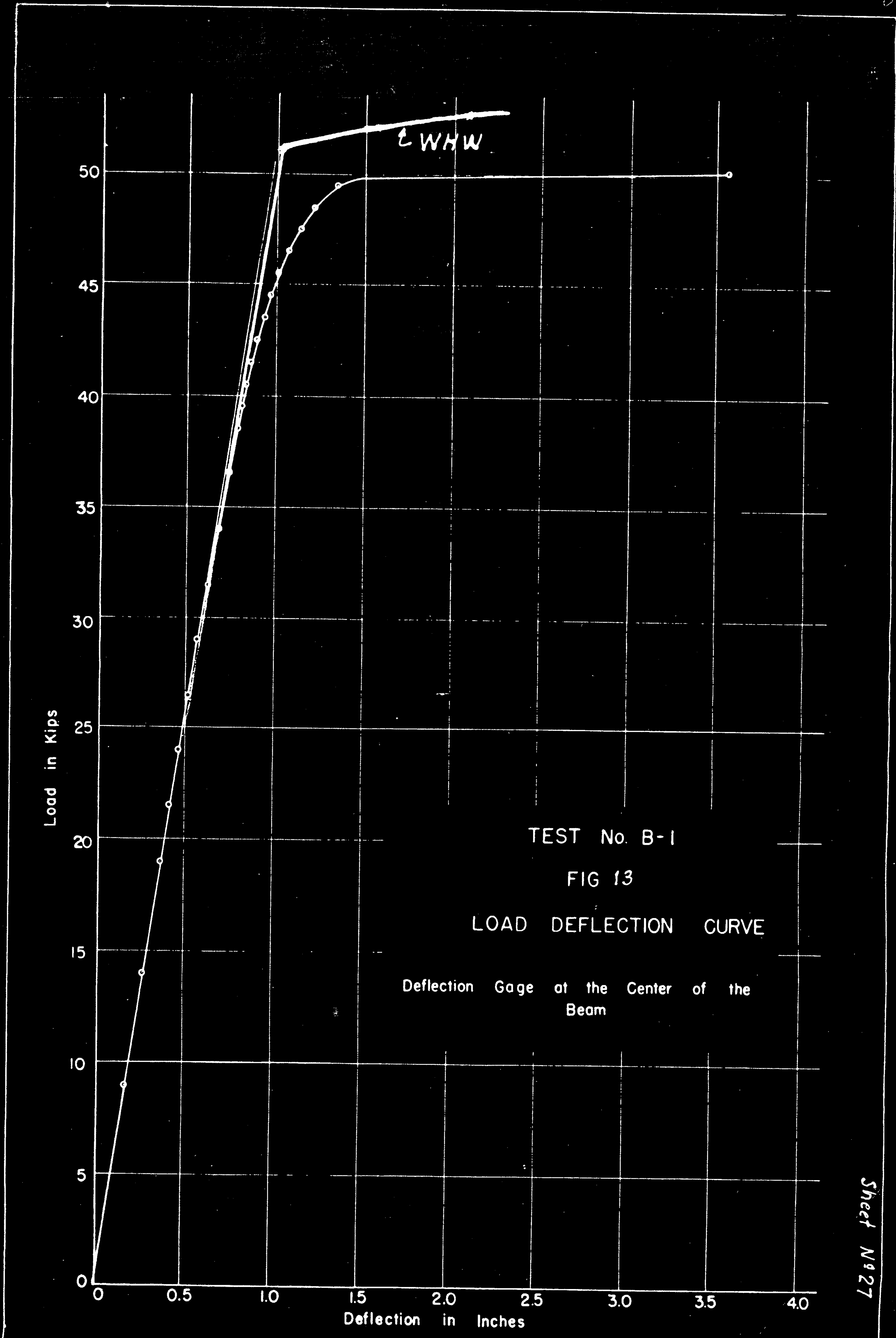

TEST No. B-1

FIG 13

LOAD DEFLECTION CURVE

Deflection Gage at the Center of the Beam

Sheet Nº 27

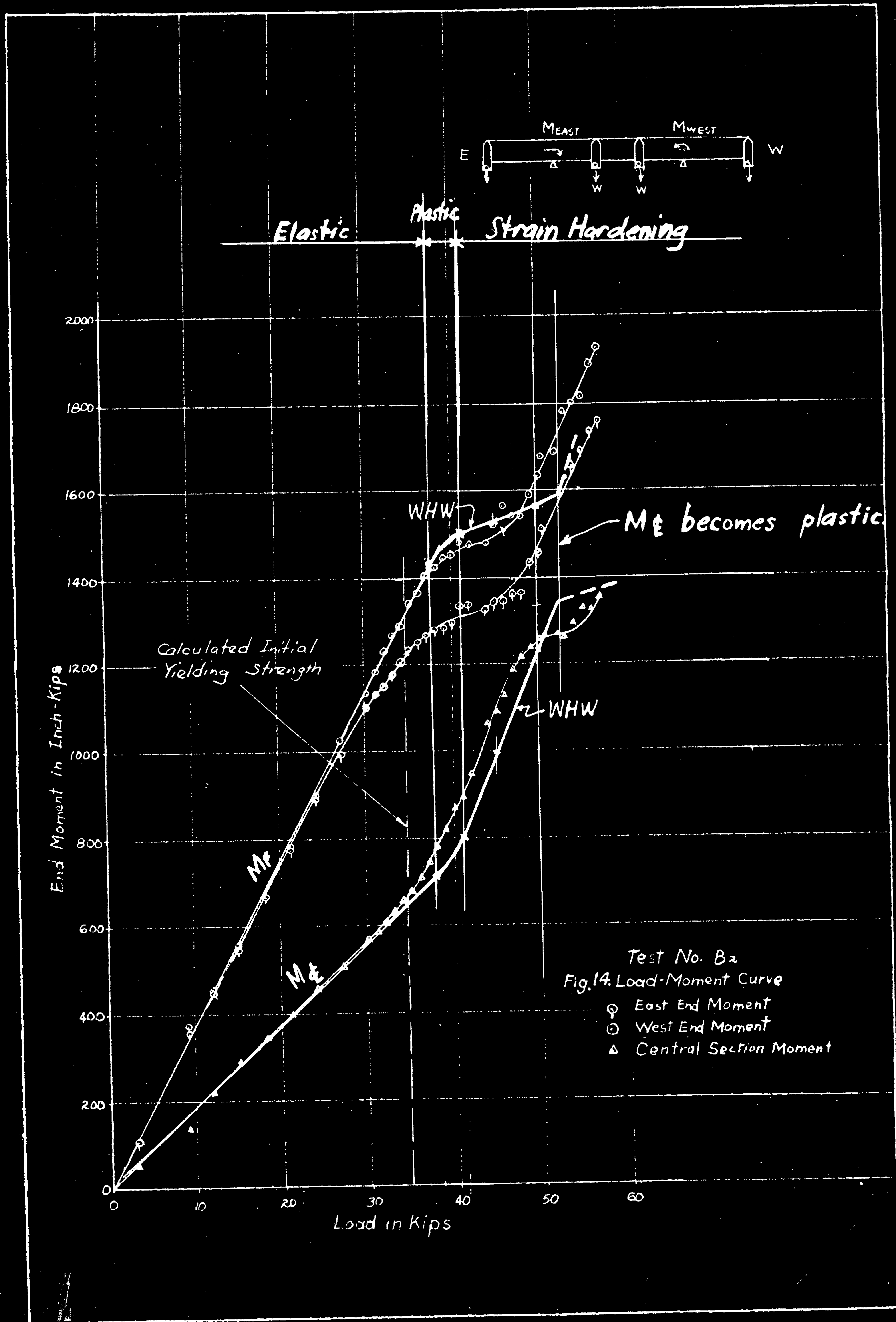

Test No. B2
Fig. 14. Load-Moment Curve

Sheet Nº 29.

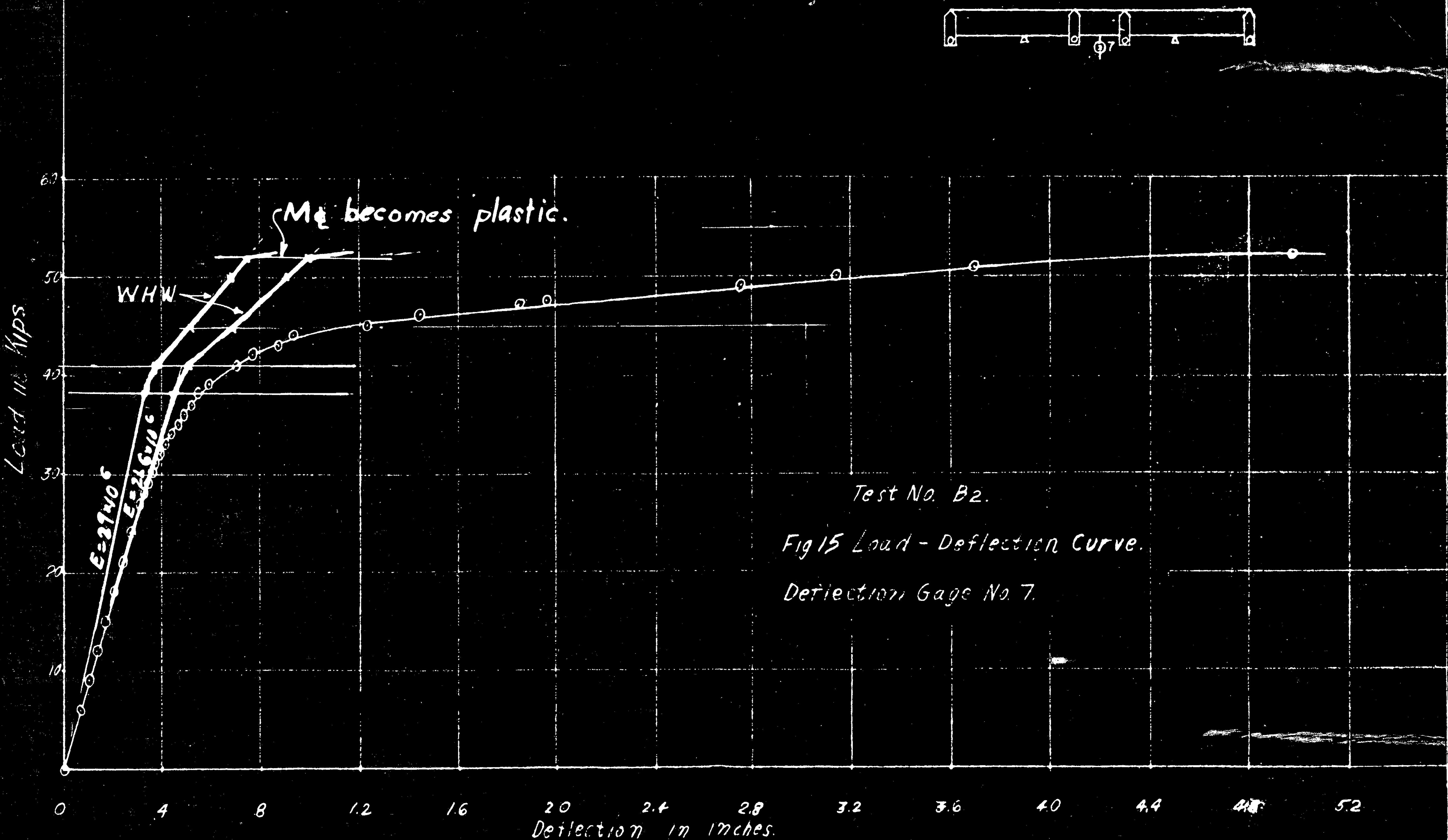

Test No. B2.

Fig 15 Load - Deflection Curve.

Deflection Gage No. 7.